Lab on a Chip

PAPER

View Article Online
View Journal | View Issue

Cite this: *Lab Chip*, 2025, **25**, 5019

A compact sample-to-answer system for rapid MRSA detection in serum based on reagent-free electrophoretic purification of nucleic acids and colorimetric LAMP

Yung Ching Lee, [a] Yang Bu,[a] Sheng Ni, [a] Yuze Liu,[b] Anni Hu[b] and Levent Yobas *[ab]

Methicillin-resistant *Staphylococcus aureus* (MRSA) poses a significant threat as a leading cause of nosocomial infections, inflicting severe complications and fatalities worldwide. Its rising prevalence has become a major public health concern as its resistance to common antibiotics complicates treatments, placing additional burden on healthcare systems. Microbial culture is the "gold standard" for diagnosing MRSA; however, this method is time-consuming and labor-intensive, often leading to prolonged delays in diagnosis and treatment. In contrast, nucleic acid amplification tests (NAATs) dramatically reduce diagnostic times to mere hours, while maintaining high sensitivity and specificity. Bringing NAATs to the point of care can facilitate timely treatment decisions and yet requires a compact "sample-to-answer" system whose development has long been hindered by the required sample preparation for these tests. Here, we present such a system detecting MRSA in human serum through a simple microfluidic chip, achieving a limit of detection of 1 CFU per reaction and a turnaround time of just 45 min. The chip effectively overcomes the sample preparation challenge with an innovative use of a sieve, a dense array of micropillars with submicrometer gaps. Along with associated reservoirs, this sieve integrates bacterial lysis, reagent-free electrophoretic purification and loop-mediated isothermal amplification (LAMP) of nucleic acids with colorimetric detection visible to the naked eye. Within the sieve, nucleic acids are selectively driven by rotating electric fields and focused near the sieve center while steady electric fields remove all contaminants, without the need for reagents. The system shows great potential for point-of-care diagnostics.

Received 14th February 2025,
Accepted 4th August 2025

DOI: 10.1039/d5lc00152h

rsc.li/loc

Introduction

A recent study predicted that by 2050, the global death toll from infections resistant to antibiotics could rise by nearly 70% approaching 40 million.[1] The same study identified that the pathogen–drug combination contributing the greatest burden across all age groups was methicillin-resistant *Staphylococcus aureus* (MRSA). For this combination—specifically the antibiotic methicillin and the bacterium *S. aureus*—the number of attributable deaths more than doubled, increasing from 57 200 in 1990 to 130 000 in 2021.[1] As such, MRSA represents a growing public health concern. MRSA is responsible for a wide range of infections, from skin and soft tissue infections to more severe conditions such as pneumonia, and bloodstream and surgical site infections.[2] Traditionally, detection of MRSA relies on microbial culture, which is the "gold standard" for pathogen detection. However, the culture-based protocol is time-consuming and labor-intensive, which frequently causes delays in diagnosis and therapeutic intervention.[3] Therefore, there is an urgent need to develop effective diagnostic tests for rapid and accurate detection of MRSA that can enable the early prevention of cross-infection among individuals and hence minimize its spread.

Diagnostic tests that can be conducted rapidly at or near the sample collection site with minimal manual intervention and prior training as well as with limited resources are known as point-of-care tests (POCTs).[4] Often referred to as "sample-to-answer" tests, POCTs are being developed for myriads of infectious diseases[5] including those caused by MRSA.[6] Among the prominent test methods, immunoassays stand out due to their simplicity, cost-effectiveness, and ability to deliver rapid results through the detection of

[a] *Department of Electronic and Computer Engineering, The Hong Kong University of Science and Technology, Clear Water Bay, Hong Kong, SAR, China.*
E-mail: eelyobas@ust.hk
[b] *Department of Chemical and Biological Engineering, The Hong Kong University of Science and Technology, Clear Water Bay, Hong Kong, SAR, China*

antibody–antigen interactions. For instance, lateral flow immunoassays have been developed for the detection of MRSA, primarily utilizing colloidal gold-labeled monoclonal antibody technology.[7,8] However, these assays have demonstrated either poor detection limits or have relied on antigenic targets that are not optimal for the method. In contrast, nucleic acid (NA) amplification tests (NAATs) are known to be much more specific and sensitive than immunoassays. Nonetheless, their implementation in POCTs has been limited due to the requirement of sample preparation, which involves the extraction and purification of NAs from target pathogens. Ideally, POCTs should achieve seamless integration of sample preparation with NA amplification techniques such as the polymerase chain reaction (PCR) or loop-mediated isothermal amplification (LAMP) to fully embody the "sample-to-answer" concept.

To this end, various NAATs have been developed for MRSA detection by implementing PCR on chips. Sista *et al.* completed a 40-cycle real-time PCR in 12 min on an electrowetting-based digital microfluidic chip by shuttling reaction droplets to a heater zone.[9] The authors performed on-chip DNA purification and elution following off-chip incubation of magnetic beads with nasal swabs carrying heat-lysed MRSA cells in lysis buffer. Shen *et al.* conducted a real-time nanoliter PCR in a 384-well SlipChip placed on an external thermal cycler and identified MRSA along with four other pathogens as low as 7 cells per well as a limit of detection (LOD).[10] Similarly, using a chip placed over a miniaturized thermal cycler, House *et al.* performed real-time PCR in microchambers (wells) and detected MRSA by amplifying a region of the 16S rRNA genes.[11] Although the authors managed to detect as low as 11.2 pg DNA in a 3 μL sample, they prepared DNA samples off chip. In a subsequent study, Oblath *et al.* integrated DNA preparation and real-time PCR on a microfluidic chip with reaction wells built on an aluminum oxide membrane wherein a saliva sample containing heat-lysed pathogens was filtered through to extract DNA.[12] The authors successfully achieved a LOD of 300 fg (100–125 copies) of both methicillin-susceptible *Staphylococcus aureus* (MSSA) and MRSA genomic DNA (gDNA) spiked into a saliva sample although most of the analysis time (>2 h) was spent on thermocycling on a Peltier stage. A comparable analysis time was reported for live MRSA detection using a PCR-based microfluidic system with an integrated micropump, microheater and temperature sensor.[13] The authors detected as low as 100 colony forming unit (CFU) per μL following on-chip thermolysis of live MRSA pathogens, followed by DNA purification through capture probes conjugated to magnetic beads.

NAATs based on isothermal amplification methods are attractive because a thermocycler is not required. Among those, LAMP has increasingly gained attention owing to its balanced performance in cost, rapidness, sensitivity and specificity.[14,15] Wang *et al.* integrated LAMP with DNA purification through probe-conjugated magnetic beads following on-chip thermolysis of MRSA pathogens in sputum, serum, and milk.[15] The study achieved a LOD of 10 fg μL^{-1} with a turnaround time of 1 h, albeit relying on a bulky spectrophotometer. Subsequently, the authors developed a smartphone-controlled portable system by adopting colorimetric LAMP, achieving an LOD of 30 CFU per reaction with a total turnaround time of 40 min, although further validation with real clinical specimens is still required.[14] Huang *et al.* identified pneumonia-related pathogens including MRSA through real-time fluorescence-based LAMP reactions performed on a centrifugal platform.[16] The diagnostic performance was validated on clinical sputum samples and achieved an LOD of 10 copies per μL with a turnaround time of 45 min although off-chip sample preparation was still required. Shah *et al.* demonstrated a USB-powered disposable printed circuit board, integrating heaters for bacterial lysis and the fluorescence-based LAMP reaction.[17] The platform was tested on clean samples, achieving an LOD of 316 genome copies in 35 min, but challenges of fluid loss during lysis at 95 °C and the automated on-chip liquid transport mechanism within the limited space remain. Choopara *et al.* presented a paper-based platform that performed on-chip amplification with fluorescence-based detection.[18] The platform achieved an LOD of 1 copy per reaction in 43 min. Although performance of detection was evaluated using blood samples spiked with 50 copies, off-chip sample preparation was still needed. A paper-based analytical device was presented by Suea-Ngam *et al.*[19] It used silver nanoplates for colorimetric detection on a paper strip using a crude lysate from pure cultures, which showed a LOD of 1 copy in 30 min. Although this paper-based system could directly perform detection using a lysate in pure cultures, purification might be required when using clinical bio-samples, where off-chip lysis and NA extraction are performed. Meng *et al.* performed multiplex LAMP assays in a chip to test positive culture of cerebrospinal fluid, which accomplished a LOD of 20 CFU per reaction in 70 min.[20] This study also required off-chip NA purification before performing on-chip analyses.

These NAATs by implementing PCR or LAMP on microfluidic chips have demonstrated high sensitivity and specificity in the detection of MRSA. However, their adoption in practical sample-to-answer systems is hampered by complicated sample preparation, *i.e.*, extraction and purification of NAs from clinical specimens. Implementing these pretreatment steps along with PCR or LAMP on microchips for an integrated analysis can be challenging and, thus, many studies could only perform off-chip sample pre-treatment without attempting to develop an integrated approach.[11,16,18–20] Solid-phase extraction (SPE), the most widely explored approach, exploits selective affinity between NAs and a solid phase.[21] However, it involves the use of several reagents in a bind–wash–elute workflow which requires fluidic valving with minimal dead volume to prevent chemical carryover between these steps. This increases not only the design and fabrication complexity but also the complications in operation.[22] Meanwhile, reagent-free NA

sample preparation concepts have been explored with the innovative use of existing techniques such as isotachophoresis (ITP),[23–25] ion concentration polarization (ICP),[26,27] entropic trapping,[28] and electrophoresis.[29–32] ITP is highly sensitive to the temperature and chemistry of the trailing and leading electrolytes, and as such requires fine tuning of the ion composition, including ion mobility, concentration, and volume, as well as pH for different samples. Similarly, ICP requires sample-by-sample calibration of an applied pressure along a microchannel for removing most contaminants while retaining NAs. Entropic trapping for NA purification has been reported albeit as a downstream process for purifying long DNA from short DNA fragments in a clean buffer.[28]

Electrophoresis can be leveraged to selectively enrich and purify NAs within a gel using rotating electric fields at a site devoid of electrodes, thereby mitigating electrochemical damage. Also known as synchronous coefficient of drag alteration (SCODA), this technique has been effectively utilized to extract DNA from oil sands, isolate DNA from humic acids,[31] and separate DNA from PCR inhibitors in forensic applications.[29] The technique, however, suffers from lengthy operation due to limited field strengths.[32] Recently, we have enhanced this technique by substituting traditional polymer gels with a microfabricated artificial sieve capable of sustaining stronger electric fields, thus reducing the operation time from hours to minutes.[22] Here, maintaining the overall design and without introducing any complexity, we further integrate NA sample preparation with upstream bacterial lysis and downstream colorimetric LAMP detection. The sieve relies on electrophoresis for sample transport and NA purification, resulting in a simple design that is free of pumps and valves and can be fabricated through a single-mask photolithographic etching process. We demonstrate its utility in a portable "sample-to-answer" system for rapid detection of MRSA pathogens in serum samples. This compact system comprises a voltage sequencer, a reaction module, a microcontroller, and a pair of color sensors (Fig. 1). Using the system, as few as 1 CFU per reaction of MRSA in serum samples can be detected within 45 min. Additionally, this system can be further upgraded to detect a broader range of pathogens in serum or similar clinical samples.

Experimental

Materials

The system is equipped with a voltage sequencer which consists of 4 compact fully programmable high-voltage supplies (uEP01-300, LabSmith, CA), a microcontroller (Arduino Uno, Italy), a customized resistive heater with a dedicated control module (Arduino Nano, Italy), an LED light source (3.3 V 3000 K-temperature LED, Jinbplight, China) and a pair of RGB color sensors (Adafruit TCS34725, NY).

Bacteria strain and mock sample preparation

The MRSA (ATCC-43300) and MSSA (ATCC-25923) strains were cultured for 24 hours in brain heart infusion broth at

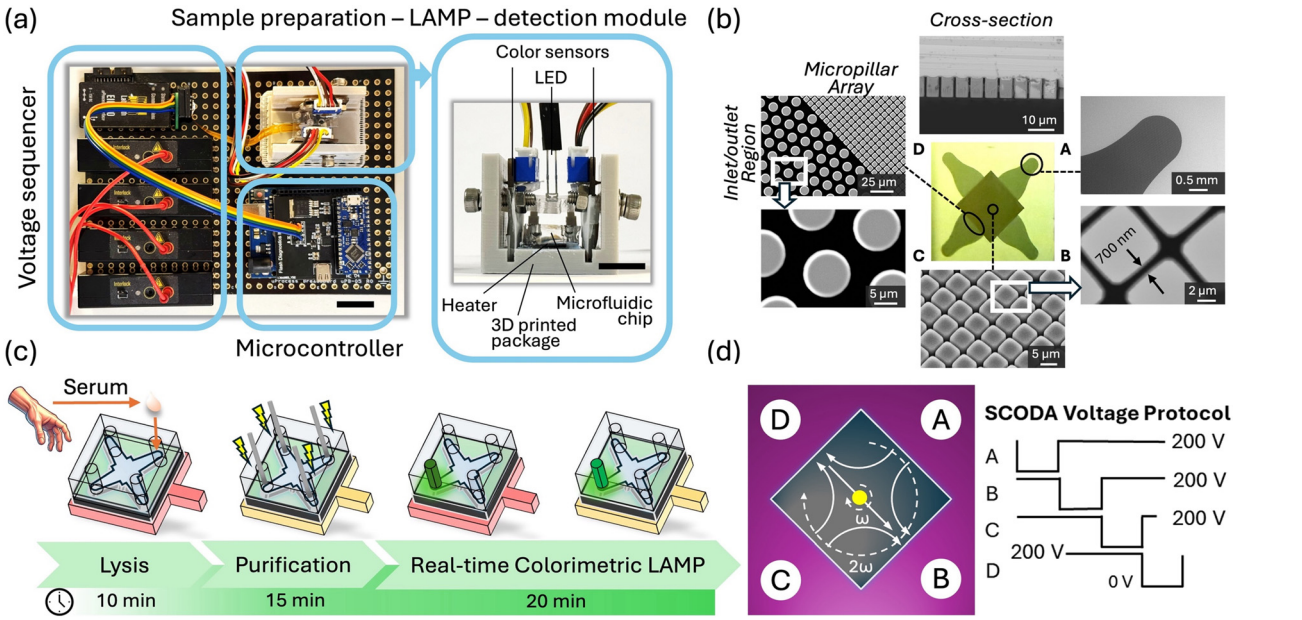

Fig. 1 (a) Top view of the system with the inset showing a side view of the reaction module where sample preparation and colorimetric LAMP detection take place (scale bars: 2 cm). (b) Top view of the microfluidic chip (the fabricated silicon substrate) along with electron microscopy images detailing various sections. (c) Schematic describing the operational workflow. (d) Illustration of the SCODA voltage protocol applied for focusing DNA. The sequential deactivation of the electrodes induces a dipole electric field rotating at ω and a quadrupole electric field rotating at 2ω across the sieve. These fields together selectively drive (focus) nucleic acids to the sieve center. Reservoir A is chosen for introducing the serum sample and lysing MRSA while reservoir C is used for collecting the purified DNA and performing the colorimetric LAMP reaction. The selection of these reservoirs can be arbitrary due to the design symmetry. The NTC reservoir is not illustrated for clarity.

37 °C. *E. coli* (ATCC-25922) was cultured for 24 h in Luria Bertani broth medium and incubated at 37 °C. The cultured MRSA was subjected to 10-fold serial dilutions, and 100 μL of each dilution was pipetted onto agar plates. The agar plates were then incubated for 24 h at 37 °C, and the number of CFU was counted based on the colonies grown on the agar plates. After determining MRSA concentrations, the bacteria were spiked into sterile-filtered serum samples from US-origin human male AB plasma (Sigma-Aldrich, MA), which were then directly loaded into the chips for subsequent analyses. Achromopeptidase (ACP, Sigma-Aldrich) was dissolved using 0.25× Tris-borate-EDTA purification running buffer (TBE, Nippon Gene, Japan). MSSA was spiked into serum and lysed by ACP in the same way as MRSA. *E. coli* was lysed by boiling for 10 min and then spiked into serum. As the input sample, 1 μL of spiked serum was added into the sieve reservoir prefilled with 9 μL of 3 U μL^{-1} ACP dissolved in 0.25× TBE buffer. Given that the input volume for the chip is fixed at 10 μL, concentrations of MRSA in the input samples can be expressed as 1000 to 0.01 CFU per reaction. The electrophoretic washing protocol was optimized by using a mock sample containing genomic MRSA DNA (ATCC-43300DQ) stained with YOYO-3 (Sigma-Aldrich) and 2 mg mL^{-1} ovalbumin (OVA) conjugated with Alexa Fluor 488 (Thermo Fisher Scientific, MA) as a contaminant in 0.25× TBE buffer.

Colorimetric LAMP assay

A 25 μL colorimetric LAMP assay included: 1 μL of 8 U μL^{-1} Bst polymerase (New England Biolabs, MA), 2.5 μL of 10× isothermal amplification buffer II (New England Biolabs), and 3.5 μL of 10 mM deoxynucleotides (New England Biolabs), 1.2 μL of 100 mM magnesium sulfate (New England Biolabs), 1 μL of 1.56 mM manganese chloride (Sigma-Aldrich), 4 μL of 2.5 mM calcein (Sigma-Aldrich), 1 μL of 6 mM hydroxynaphthol blue (Macklin, China), 2.5 μL of a 10× primer set that includes 16 μM forward internal primer, 16 μM backward internal primer, 2 μM F3 primer, 2 μM B3 primer, 8 μM loop forward primer, and 8 μM loop backward primer (Integrated DNA Technologies, IA), 1.5 μL of pathogen sample, and 6.8 μL of DNase-free deionized water (Invitrogen, CA). The sequences of the primers are listed in Table S1.

Chip fabrication

The major process steps are illustrated in Fig. S1a. A 4 inch, single-sided polished silicon wafer was first deposited with a low-temperature oxide (LTO) layer of 2 μm thick. The wafer was then spin-coated with a photoresist (504, Fujifilm, Japan) of 1 μm thick and then subjected to photolithography to outline the sieves. The exposed LTO was etched using advanced oxide etching (AOE), leaving a patterned oxide as a hard mask for subsequent silicon etching. The sieves were formed through silicon deep reactive ion etching (DRIE), with the pillar height determined by the number of etching cycles. The pillar-to-pillar spacing was tuned in the range of 200 to 1100 nm by uniformly growing a thin layer of wet oxide. Using oxygen plasma treatment, each fabricated chip was bonded to a 5 mm-thick PDMS slab featuring five holes with a diameter of 3 mm. Once bonded, these holes served as reservoirs with four reservoirs connected to the sieve and an additional isolated reservoir designated for the no-template control (NTC). Each chip was filled with a 0.25× Tris-borate-EDTA working buffer containing 0.5% v/v performance optimized polymer (POP)-6 (Applied Biosystems, CA) to suppress electroosmosis. Bubbles were expelled from the sieve using electrophoresis in a 10 min pre-run induced by platinum wire electrodes (Leego Precision Alloy, China) immersed in the sieve reservoirs and sequentially pulsed at 300 V_p for 100 s. The chip was then placed on a customized resistive heater, with a layer of thermal grease (Kafuter, China) at the interface.

Results and discussion

System overview

An overview of the entire system is shown in Fig. 1a. The system has a footprint comparable to the size of a small tablet. Nearly half of this space is occupied by a programmable high-voltage sequencer which consists of four units with each unit capable of delivering up to 300 V. This sequencer can be further scaled down in the final prototype where only a fixed voltage level is needed. The remaining space is shared between a microcontroller and the reaction module housing a microfluidic chip where sample preparation and colorimetric LAMP detection take place. The module is equipped with a customized resistive heater for temperature control during bacterial lysis and the LAMP reaction, an LED light source for illumination and a pair of RGB color sensors for colorimetric detection, with one sensor assigned to the target reaction reservoir and the other to the NTC reservoir. For every sample to be analyzed, the module is provided with a pristine microfluidic chip filled with the running buffer. The chip rests on the customized resistive heater regulated by a proportional-integral-derivative (PID) feedback controller (Fig. S1b and S2). The temperature profile of the heated solution in the chip reservoir can remain stable for over 20 min, with fluctuations limited to less than ±1 °C (Fig. S3).

Microfluidic chip

Fig. S1b presents an exploded description of the reaction module housing the microfluidic chip. The microfluidic chip is built on a silicon substrate featuring a dense array of oxidized silicon micropillars serving as an artificial sieve for SCODA focusing and reagent-free purification of nucleic acids from a sample lysate. The array is enclosed from above with a PDMS cover (irreversibly bonded to the silicon substrate) and accessed through four inlet/outlet reservoirs built into the cover. These reservoirs are held at electrical potentials defined by a voltage sequencer through platinum wire electrodes mounted on a PDMS manifold and placed

over the microfluidic chip. The symmetrical design allows any pair of the four reservoirs to be used for lysing the sample and then collecting the purified DNA for the subsequent LAMP. Transport between these reservoirs and the sieve is realized by electrophoresis. Adjacent to the LAMP reservoir is the NTC reservoir (not illustrated), which is isolated from the sieve and contains reagents but no template.

Fig. 1b depicts the fabricated silicon chip without a PDMS cover. The chip features a 5 mm-by-5 mm two-dimensional sieve composed of square oxidized silicon micropillars that are 5 μm wide, 10 μm tall, and spaced apart by 700 nm. This spacing remains uniform across the entire wafer, with a mean value of 726 ± 33 nm (n = 6), which is crucial for the electrophoretic purification of DNA. The cross-sectional view of the sieve confirms that the pillars have a height of 10 μm. The sieve access channels including the reservoirs are populated with 10 μm circular pillars situated at a pitch of about 15 μm to prevent potential clogging as well as the collapse of the PDMS cover.

Operational workflow

Fig. 1c briefly describes the operational workflow. Initially, the microfluidic chip is filled with a running buffer and a serum sample containing MRSA pathogens is loaded into the sieve reservoir that contains ACP enzyme. The mixture is incubated at an elevated temperature for an increased enzyme activity and effective lysis. Subsequently, nucleic acids and other negatively charged species present in the lysate are introduced into the sieve through electrophoresis. The reagent-free electrophoretic purification of nucleic acids from contaminants involves sequentially deactivating the electrodes. This consequently leads to focusing and enrichment of the nucleic acids at a site near the sieve center while effectively clearing contaminants from the sieve. Once purified, the nucleic acids are transported to the reaction reservoir. Finally, the LAMP reaction is conducted in the reservoir at an elevated constant temperature after adding the required reagents. The test result is obtained *via* real-time colorimetric detection.

The underlying principle of DNA purification through SCODA focusing has been elaborated in earlier studies.[30,31] Briefly, the method involves the simultaneous application of a uniform dipole electric field rotating at a specific angular frequency (ω) and a quadrupolar electric field oscillating at twice that frequency (2ω). Unlike most molecules, which exhibit a relatively constant electrophoretic mobility, DNA demonstrates an electrophoretic mobility that varies linearly with the electric field, as predicted by the biased reptation with a fluctuation model[33] and confirmed through agarose gel electrophoresis.[34] This field dependence results in a quadratic relationship between DNA velocity and the applied field strength. Consequently, when a dipole field rotates at frequency ω, it generates a velocity component oscillating at 2ω. Simultaneously applying a mobility-modulating quadrupole field rotating at 2ω induces an average drift velocity that directs the DNA toward the center of the field pattern. This radial drift is crucial for focusing the DNA and is influenced by the strengths of the dipole and quadrupole fields, as well as the distance of the DNA from the center of the field.

Fig. 1d describes the voltage protocol employed, which involves deactivation of all four electrodes one at a time in sequence to induce these rotating dipole and quadrupole fields. Notably, these fields exert no net drift on contaminants with field-independent mobility; such contaminants merely move in circular paths under zero time-average fields. Therefore, they must be cleared from the sieve, which is implemented here through electrophoretic washing. Table 1 outlines the full sequence of voltage levels delivered to the electrodes for sample injection and DNA focusing, as well as the subsequent contaminant removal (electrophoretic washing) and DNA collection. The DNA focusing is realized by looping four sequential steps for about 3 min with each step lasting 0.5 s. Subsequent removal of contaminants is performed by repeatedly applying 3 s electrophoretic washing alternated with 1 min refocusing (10 repeats).

On-chip MRSA lysis

Unlike Gram-negative bacteria such as *E. coli*, which can be lysed by boiling, MRSA requires the use of lytic enzymes.[35] MRSA is a Gram-positive bacterium with a thick peptidoglycan cell wall, which poses significant challenges for lysis compared to other bacterial species. This thick cell wall structure provides inherent resistance to bacteriolytic enzymes such as lysozyme. Therefore, ACP was selected to lyse MRSA, which is a blend of proteases and peptidoglycan-specific hydrolases and has been proven to be an effective bacteriolytic enzyme for Gram-positive bacteria like *S. aureus*.[36]

The effectiveness of on-chip lysis is assessed by examining the size and intensity of bright spots of YOYO-stained MRSA DNA near the sieve centre following the sample injection and 3 min of SCODA focusing. These spots are compared across various incubation temperatures and periods, and ACP concentrations for 1 μL serum samples spiked with 100 CFU

Table 1 The full sequence of voltage levels delivered to the electrodes for sample injection, DNA focusing, contaminant removal (electrophoretic washing) and DNA collection

Sequence\electrode	A	B	C	D
Injection (1 min)	0 V	200 V	200 V	200 V
Focusing steps (0.5 s each) looped for 3 min	0 V	200 V	200 V	200 V
	200 V	0 V	200 V	200 V
	200 V	200 V	0 V	200 V
	200 V	200 V	200 V	0 V
Washing (3 s) alternated with refocusing (1 min) repeated for 10 cycles	200 V	200 V	0 V	200 V
Collection (1 min)	0 V	200 V	200 V	200 V

per reaction of MRSA (Fig. 2). As shown in Fig. 2a, incubation at room temperature is ineffective due to the inactivity of the enzyme at this temperature, resulting in a predominantly punctuated fluorescence pattern near the sieve centre, indicative of intact MRSA pathogens. In contrast, the incubation at elevated temperatures of 37 °C and 56 °C yields a diffused spot signifying extracted DNA with very few intact MRSA pathogens remaining. Raising the incubation temperature to 65 °C significantly reduces both the spot size and the number of intact pathogens. The spot intensity increases with prolonged incubation as demonstrated by the results for varying incubation periods at 37 °C as shown in Fig. 2b. 30 min incubation is optimal, while 5 min incubation appears insufficient; 10 min incubation is acceptable, producing a small but noticeable spot. Throughout these trials, the ACP concentration is maintained at 2.7 U μL^{-1}, which has proven effective based on the results from 20 min incubation at 37 °C (Fig. 2c). Lower or higher ACP concentrations yield barely noticeable spots, with higher concentrations leading to DNA degradation.[36] Based on these findings, the lysis protocol is established as 10 min incubation with 2.7 U μL^{-1} ACP at 37 °C.

Reagent-free DNA purification

Reagent-free DNA purification relies on selective enrichment of nucleic acids near the sieve center under SCODA focusing. Our previous study[22] has shown that various factors play a major role in the enrichment speed including the pillar-to-pillar spacing along with operating conditions such as the peak voltage, step time, and buffer ionic strength. While we initially assessed these factors using pure λDNA samples and sieves with circular micropillars, we further explore here their impact on the focusing of MRSA DNA extracted from serum samples spiked with MRSA pathogens, utilizing sieves with square micropillars (Fig. 1b). Fig. 3 presents the time traces of fluorescence intensity levels (averaged within the focused spot near the center of the sieve and normalized by the spot area), illustrating the focusing dynamics of YOYO-stained MRSA DNA at the specified pillar-to-pillar distance, peak voltage, step duration, and buffer ionic strength. The traces exhibit an increasing trend over time. Under select conditions, they reach saturation within 3 min of focusing, which justifies the selection of this duration for looping the focusing steps of the voltage protocol in Table 1. Fig. S4 displays the fluorescence images of the corresponding spots captured after 3 min of focusing.

Fig. 3a reveals that a submicrometer sieve is crucial for the effectiveness of the method as a 700 nm sieve leads to a more prominent focused spot of YOYO-stained MRSA DNA compared to 900 nm or 1.1 μm sieves. In such coarse sieves, the field strengths are insufficient to drive DNA electrophoresis under the same peak voltage. However, further reducing the critical sieve size to 500 nm, while it increases the field strength, leads to a much less prominent spot primarily due to the difficulty of injecting large DNA molecules into such fine sieves under a steep entropic barrier. Likewise, no visible spot is encountered in a 200 nm sieve as most DNA molecules are unable to enter the sieve (not shown). Reducing the peak voltage (Fig. 3b) and increasing the ionic strength of the working buffer (Fig. 3c) also lead to reduced field strengths which can negatively impact the focusing process. Maximum enrichment can be attained by activation at 200 and 300 V_p although the latter leads to a relatively steep focusing trace. Meanwhile, it may

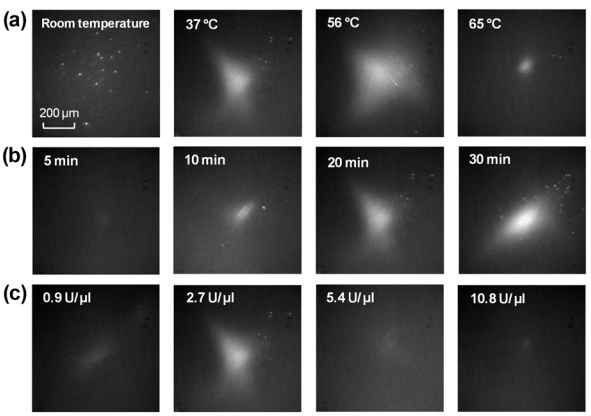

Fig. 2 Fluorescence images of YOYO-stained MRSA DNA spots after 3 min SCODA focusing across 700 nm sieves with sample injection following on-chip lysis. The images show the effectiveness of on-chip lysis achieved by incubating 1 μL serum samples spiked with 100 CFU per reaction of MRSA with the enzyme ACP for various incubation (a) temperatures and (b) durations, as well as (c) ACP concentrations with respective values at 37 °C, 20 min, and 2.7 U μL^{-1}, unless otherwise stated. The voltage protocol applied is as outlined in Table 1.

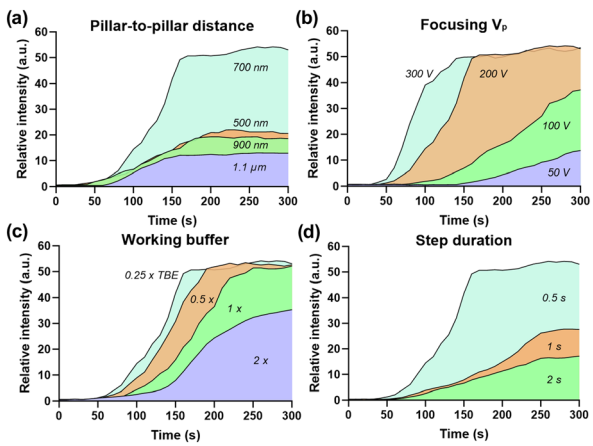

Fig. 3 Time traces of averaged and normalized fluorescence intensity levels of YOYO-stained MRSA DNA spots near the sieve center during SCODA focusing with sample injection following on-chip lysis (1 μL serum samples spiked with 100 CFU of MRSA incubated with 2.7 U μL^{-1} ACP at 37 °C for 10 min). The traces show the effectiveness of SCODA focusing at the stated (a) pillar-to-pillar distance, (b) peak voltage V_p, (c) working buffer strength, and (d) step duration. Unless otherwise stated, the SCODA focusing takes place across a 700 nm sieve filled with 0.25× TBE buffer, utilizing a peak voltage of 200 V_p and a step duration of 0.5 s.

take longer to reach saturation with an increased step duration (Fig. 3d) because of the lengthened trajectory of DNA in reaching the focusing point. The DNA oscillates while drifting toward the sieve center and the oscillations become larger with increasing step duration.[21] Based on these results, the subsequent experiments used a 700 nm sieve filled with 0.25× TBE and activation at 200 V_p applied for a step duration of 0.5 s.

Fig. 4a shows the spots of YOYO-stained MRSA DNA near the center of 700 nm sieves after 3 min SCODA focusing following on-chip lysis and injection of serum samples spiked with varying concentrations of MRSA pathogens. At 1000 CFU per reaction, a relatively large, focused spot emerges along with intact MRSA pathogens possibly due to inadequate ACP enzyme concentration. At 100 CFU per reaction, the spot remains focused but appears smaller with no intact pathogen detected. As the concentration decreases to 10 and 1 CFU per reaction, the spots become increasingly diffuse, ultimately becoming indistinguishable at 0.1 CFU per reaction (not shown). In Fig. 4b, the corresponding time traces of averaged and normalized fluorescence intensity levels illustrate the focusing dynamics across different MRSA concentrations. Movie S1 shows the SCODA focusing of MRSA DNA from serum samples spiked with 10 and 100 CFU per reaction.

As the sample injection into the sieve is through electrophoresis, only negatively charged contaminants present in the serum lysate can enter the sieve and yet need to be removed before transporting the focused DNA to the reaction reservoir for the colorimetric LAMP detection. This removal is achieved through a cyclic process alternating electrophoretic washing and SCODA focusing. This approach preserves the concentrated DNA near the sieve center through a refocusing mechanism driven by the voltage protocol outlined in Table 1. Fig. 5 demonstrates this process using a mock sample containing the YOYO-stained genomic DNA of MRSA and Alexa-stained OVA, representing contaminants (Movie S2). In Fig. 5a, the 700 nm sieve is shown filled with OVA co-injected with MRSA DNA, which remained uniformly distributed after 3 min of SCODA focusing. Fig. 5b displays the sieve progressively cleared of OVA during the electrophoretic washing steps. In Fig. 5c, the focused DNA spot is observed migrating away from the sieve center during a washing step, only to be brought back by the subsequent refocusing. This washing–refocusing cycle is repeated ten times to ensure the removal of most contaminants from the sieve. Finally, Fig. 5d shows the purified MRSA DNA driven to the collection reservoir by electrophoresis for the subsequent LAMP reaction.

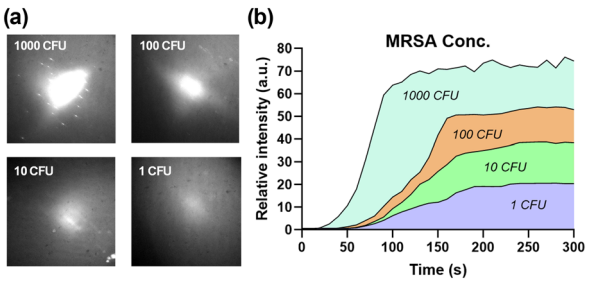

Fig. 4 (a) Fluorescence images of YOYO-stained MRSA DNA spots near the sieve center after 3 min SCODA focusing with sample injection following on-chip lysis (1 μL serum samples spiked with MRSA pathogens incubated with 2.7 U μL^{-1} ACP at 37 °C for 10 min). The images show the effectiveness of SCODA focusing across 700 nm sieves using serum samples spiked with decreasing MRSA concentrations, ranging from 1000 to 1 CFU per reaction. (b) Corresponding time traces of averaged and normalized fluorescence intensity levels of YOYO-stained MRSA DNA spots near the sieve center. The voltage protocol applied is as outlined in Table 1.

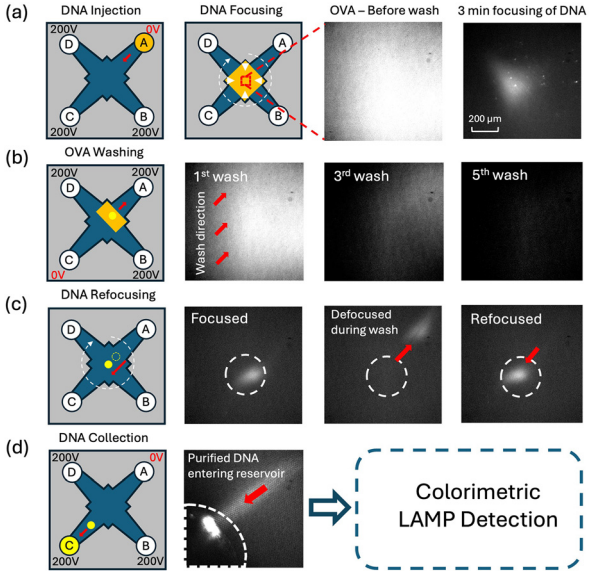

Fig. 5 Illustrations and fluorescence images describing the reagent-free purification of MRSA DNA across a 700 nm sieve, which involves the selective enrichment of nucleic acids near the sieve center under SCODA focusing, the subsequent removal of contaminants from the sieve while retaining the focused DNA, and then the collection of purified DNA into a reservoir for the LAMP reaction and colorimetric detection. Fluorescence images: (a) the distribution of Alexa-stained OVA and YOYO-stained MRSA genomic DNA near the sieve center after 3 min of SCODA focusing; (b) the gradual removal of OVA from the sieve during electrophoretic washing steps, following the voltage protocol outlined in Table 1; (c) YOYO-stained MRSA DNA focused into a spot near the sieve center (dashed circle) leaving the spot during electrophoretic washing and then returning during the subsequent SCODA focusing (refocusing); (d) YOYO-stained MRSA DNA entering the collection reservoir for the subsequent LAMP reaction. The washing–refocusing cycles (10 repeats) lead to the removal of most contaminants co-injected with nucleic acids from the sieve.

Colorimetric LAMP

The choice of LAMP over PCR avoids the requirement of a thermocycler, which is crucial for creating a simple point-of-care system. Further simplicity arises from visual colorimetric dyes that can be added into the LAMP mixture and enables the readout of LAMP results based on a color change noticeable to the naked eye. For the colorimetric LAMP

detection, the two most common dyes are calcein and hydroxynaphthol blue (HNB).[37,38] Although the two dyes are applied separately, their mixture enhances the colorimetric effect, allowing for better differentiation between positive and negative results under natural light conditions, which may not be obvious if either dye is used alone.[39] Calcein and HNB are both metal ion indicator dyes, with calcein forming a complex with Mn^{2+} ions, resulting in an orange color, and HNB forming a complex with Mg^{2+} ions, producing a violet color. During LAMP, pyrophosphate by-products from DNA synthesis react with divalent ions such as Mg^{2+} and Mn^{2+}, forming insoluble compounds. In this process, calcein and HNB gradually release the metal ions, causing a color change from orange to yellow in the case of calcein, and from violet to sky blue in the case of HNB.

Specific proportions of the two dyes in combination with the concentrations of Mg^{2+} and Mn^{2+} ions need to be tuned before implementing LAMP on chip. Fig. S5a shows the endpoint LAMP results obtained using MRSA lysates (without serum) with calcein concentrations varying from 100 to 800 μM while keeping the HNB concentration at 240 μM. At lower concentrations (100 and 200 μM), MRSA-positive samples exhibit a blue color whereas MRSA-negative samples display a violet color, consistent with previous findings.[39] Increasing the calcein concentration to 400 μM results in a vibrant bright green color for MRSA-positive samples as opposed to a brown color for negative samples. This concentration provides a sufficient contrast to effectively distinguish between positive and negative results. Notably, this allows for detecting a MRSA level as low as 1 CFU per reaction based on the LAMP results from 10-fold serial dilutions of a MRSA lysate (ranging from 1000 to 0.01 CFU per reaction) as presented in Fig. S5b.

To achieve rapid and high-contrast colorimetric detection using a calcein and HNB mixture, it is crucial to optimize the concentrations of Mg^{2+} and Mn^{2+} ions. A concentration of Mg^{2+} below 4 mM significantly hampers the activity of Bst DNA polymerase, thereby impeding DNA synthesis.[40] Raising the Mg^{2+} concentration to 4.8 mM in our experiments produces vibrant bright green and brown colors for positive and negative samples, respectively, within a 20 minute LAMP reaction using the MRSA lysate. This concentration not only shortens the detection time but also enhances the contrast of the colorimetric results. Conversely, higher concentrations of Mg^{2+} (6 and 8 mM) extend the detection time to over 30 min. This delay can be attributed to the prolonged depletion of free Mg^{2+} ions during the LAMP reaction, as an excess of Mg^{2+} in the assay slows down the release from the HNB–Mg^{2+} complex, postponing the observable color change.[37] The role of Mn^{2+} is primarily to influence the color as well as the duration of the color change observed in calcein. At a low concentration of 31.3 μM, no significant color differentiation is noted between positive and negative samples; both appear close to green when tested with the MRSA lysate. This lack of distinction arises from an insufficient amount of Mn^{2+} ions to quench calcein's green color.[41] Increasing the Mn^{2+} concentration to 62.5 and 125 μM yields the most pronounced color change, with positive samples exhibiting a bright green color and negative samples displaying a brown color. Notably, the 62.5 μM concentration produces this result within just 20 min, which is twice as fast as the 40 min required at 125 μM. The longer duration at the higher concentration is likely due to the excess Mn^{2+} ions, which prolong the time needed for pyrophosphate by-products from DNA synthesis to deplete the calcein–Mn^{2+} complex, thus delaying the release of the green hue in calcein.[41] Consequently, we selected 4.8 mM Mg^{2+} and 62.5 μM Mn^{2+} for the subsequent on-chip LAMP experiments.

The optimal temperature for LAMP varies among different pathogens,[42] necessitating adjustments for MRSA to minimize detection time. Within the temperature range of 60 °C to 67 °C, a temperature of 62 °C yields a detectable color change in just 20 min using the MRSA lysate (100 CFU per reaction) with optimized dye and ion concentrations. This is significantly faster than other temperatures, which typically require 25 to 60 min to achieve colorimetric results. Consequently, 62 °C has been selected as the optimal LAMP temperature for the subsequent experiments.

These results are reproducible when performed on chip with a 10 μL LAMP reagent mix and MRSA DNA purified through SCODA focusing across 700 nm sieves with sample injection following on-chip lysis of serum samples. Fig. 6a shows the endpoint results from the reaction and NTC reservoirs after a 20 min LAMP run at 62 °C, using serum samples spiked with varying levels of MRSA pathogens. Expectedly, positive results exhibit a vibrant bright green color with the color tone proportional to the MRSA level in serum, whereas the NTC reservoirs display a gray or brownish color. The color change is discernible for MRSA levels as low as 1 CFU per reaction, indicating a LOD of 1 CFU per reaction, which is comparable to or lower than previously reported values (Table S2). In Fig. 6b, signals generated by the color sensor (green channel) indicate that the color change in these reservoirs begins as early as 12 min into the LAMP reaction, reaching saturation intensity within the subsequent 3 to 8 min. The normalized signal levels at 20 min correlate well with the MRSA level as illustrated in the bar chart in Fig. 6c.

Lastly, the versatility of the system for detecting the presence of other pathogens in serum by simply using an appropriate primer set is shown in Fig. 6d. The choice of primer set is crucial for determining detection specificity. For instance, the *mec*A gene is highly specific to the methicillin-resistant protein found in MRSA and is absent in other *S. aureus* strains, such as MSSA.[43] Thus, the *mec*A primer set can be used to selectively identify MRSA against MSSA or *E. coli* in serum, facilitating timely and appropriate treatment for MRSA infections in patients colonized with *S. aureus*. The selectivity for MRSA can be further seen in signals generated by the color sensor (green channel) presented in Fig. 6e. In contrast, the primer set targeting the *spa* gene cannot differentiate between MRSA and MSSA,

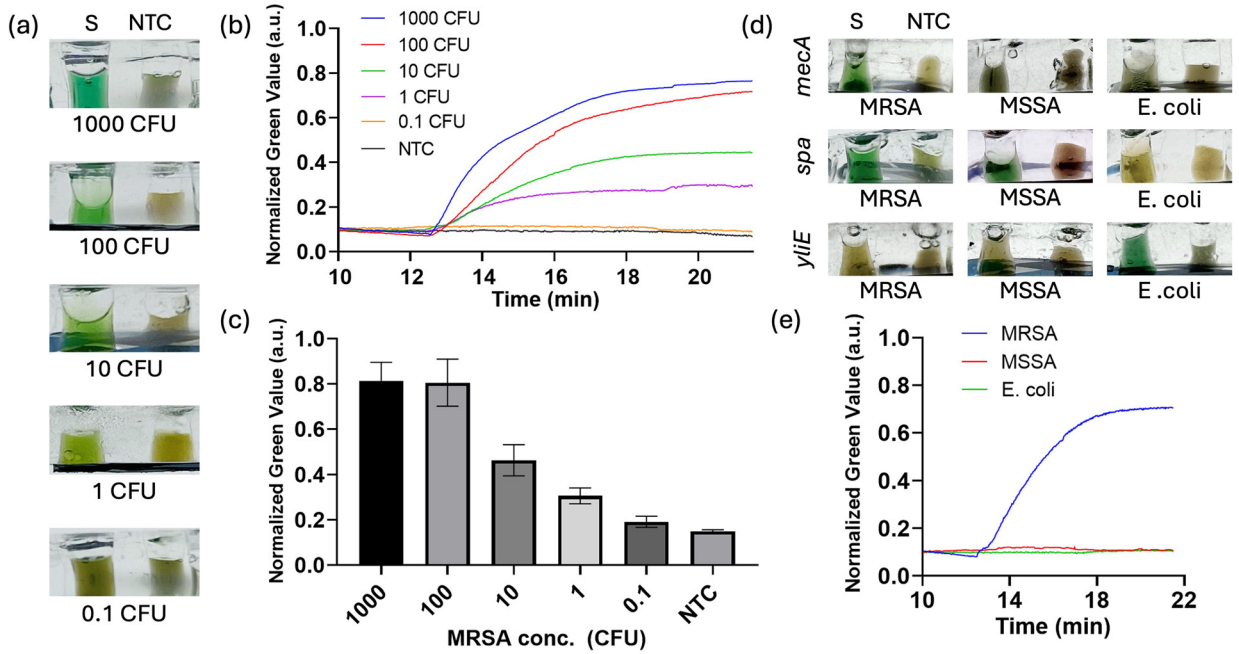

Fig. 6 (a–c) Results of on-chip colorimetric LAMP reactions (62 °C) targeting MRSA DNA purified through SCODA focusing across 700 nm sieves with sample injection following on-chip lysis. (a) Side view images of the reservoirs containing purified nucleic acids (S) from serum samples spiked with the stated MRSA concentrations in CFU as well as no template controls (NTC) shown after 20 min LAMP reactions. (b) Plot of temporal signals obtained from these reactions by the color sensors (green channel). (c) Bar chart of the mean signal values reached after 20 min LAMP reactions with error bars indicating standard deviations based on triplicates. (d and e) Specificity of pathogen detection through on-chip colorimetric LAMP with primer sets specific to genes (upper) *mecA*, (middle) *spa*, and (lower) *yliE* targeting MRSA, MSSA and *E. coli* (100 CFU per reaction) DNA purified through SCODA focusing across 700 nm sieves with sample injection following lysis. (d) Side view images of the reservoirs containing purified nucleic acids (S) from serum samples spiked with the stated pathogens as well as no template controls (NTC) with the images captured after 20 min reactions (62 °C). (e) Plot of temporal signals (green channel) obtained from the corresponding on-chip LAMP reactions with a primer set specific to the *mecA* gene. Lysis: on-chip incubation of 1 μL serum samples containing MRSA or MSSA with 2.7 U μL^{-1} ACP at 37 °C for 10 min, while off-chip boiling of 1 μL serum samples containing *E. coli* for 10 min.

as this gene is expressed by both strains although it can still be used to detect *S. aureus* in the presence of *E. coli*. *E. coli* can be selectively identified using the *yliE* gene primer against *S. aureus*.

Conclusions

We have presented a compact "sample-to-answer" system for the detection of MRSA bacteria in human serum, achieving a LOD of 1 CFU per reaction and a turnaround time of just 45 min. Our system delivers performance on par with the most advanced platforms, which are listed in Table S2, while requiring minimal sample volumes, a key advantage for paediatric patients who often have limited blood samples available. The system achieves this through a simple microfluidic chip that seamlessly integrates bacterial lysis, reagent-free electrophoretic nucleic acid purification, and colorimetric LAMP detection. This integration is primarily driven by a microfabricated sieve that facilitates the selective focusing and enrichment of nucleic acids towards its center through rotating electric fields while removing contaminants through steady fields. This innovative approach eliminates the need for reagents typically used in traditional methods and avoids the associated complexities such as flow control and reagent storage, thereby simplifying the design, which is attractive for point-of-care settings. Further simplicity arises from the use of LAMP, which does not require a thermocycler, and the use of a colorimetric readout that relies on inexpensive color sensors instead of sophisticated optics.

In comparison with the studies in Table S2, which rely on off-chip lysis, commercial extraction kits, or complex magnetic bead procedures, our system innovatively integrates on-chip bacterial lysis with a reagent-free nucleic acid purification method based on electrophoresis. As a result, all steps can be performed within a fully automated, compact device. While some studies utilize PCR and fluorescence-based detection, our approach simplifies the process by using LAMP, which eliminates the need for a thermocycler, and a colorimetric readout that can be measured with inexpensive color sensors rather than complex optics.

Handheld and compact systems for *S. aureus* detection are rare due to the significant challenges of integrating both sample preparation and detection units in a limited space. Of the systems listed in Table S2, only those by Ma *et al.*[14] and Shah *et al.*[17] qualify as handheld; however, they either require larger sample volumes, lack fully integrated nucleic acid purification, or have only been validated with clean samples.

In contrast, our system effectively addresses these limitations by streamlining the workflow, enabling rapid sample-in-answer-out detection from serum samples.

Thus, the system holds great potential for widespread deployment in hospitals and clinics, bolstering efforts in the fight against MRSA. To this end, several limitations must be overcome. First, serum needs to be isolated from whole blood beforehand. However, compared to nucleic acid extraction and purification, this preparation is relatively straightforward; it can be realized using simple tools. A hand-powered fidget spinner, previously demonstrated for blood plasma separation[44] and subsequently pathogen enrichment in urine[45] can be further adopted here. Second, the LOD of 1 CFU per reaction achieved here, while it is on par with the state of the art (Table S2), corresponds to a concentration of 1000 CFU per mL blood. While this detection level is within the range encountered in bloodstream infections (BSIs), which typically spans from 1 to 10^4 CFU per mL blood,[46] and is generally elevated in pediatric patients,[47] some early stages of BSIs can present with levels below 1 CFU per mL blood.[48,49] This limitation can be addressed by adopting pathogen enrichment strategies commonly used in molecular diagnostics, allowing for the detection of BSIs without the need for blood cultures.[50] As the required sample volume for analysis is just 1 μL—an order of magnitude lower than that of most existing platforms (Table S2)—it is feasible to detect relatively low BSI levels using an appropriate enrichment factor from typical blood collections. Additionally, the system can be used alongside blood cultures to shorten the time required for blood culture positivity. Future efforts will focus on addressing these limitations, validating the system with clinical samples and expanding its capabilities to target additional antibiotic-resistant pathogens. The assay duration can be further reduced by accelerating amplification through "hot" electron injection as a result of nanoplasmonics that can be integrated into the reservoir.[51]

The simultaneous detection of various causative species of BSIs should be carried out in a single assay. While LAMP has limited multiplexing capabilities, microfluidic reactions for target species can be carried out in parallel within dedicated reservoirs, using templates delivered through fluidic channels that are designed to minimize cross contamination.[52] This approach complements other known methods to enhance multiplexing LAMP including those that use modified primers, universal probes, restriction enzymes, nanoparticles and techniques like melting curve analysis.[53] In our design, two of the reservoirs dedicated to delivering voltage pulses can also be utilized for LAMP targeting additional species. More species can be targeted by increasing the number of reservoirs around the sieve; however, this may require smaller reservoirs and/or a larger sieve. The latter would necessitate higher voltage levels. Additionally, a suitable voltage protocol must be developed to effectively distribute purified templates to these reservoirs.

Lastly, the microfluidic chip is fabricated through a relatively straightforward process using only one-mask photolithography and standard tools available in many chip foundries worldwide. To lower the cost, however, the silicon base can be replaced with a replica-moulded PDMS substrate (Fig. S6).

Author contributions

Conceptualization: L. Y., Y. B. and Y. C. L. Methodology: L. Y., Y. B., Y. C. L., S. N., Y. L. and A. H. Validation: Y. B., Y. C. L., S. N., Y. L. and A. H. Formal analysis: Y. C. L. Writing – original draft, review & editing: L. Y., Y. B. and Y. C. L. Supervision, resources, project administration and funding acquisition: L. Y.

Conflicts of interest

There are no conflicts to declare.

Data availability

Supplementary information available: SI movies, figures and tables. See DOI: **https://doi.org/10.1039/D5LC00152H**

The data supporting this article have been included as part of the SI.

Acknowledgements

This project was financially supported by the Center on Smart Sensors and Environmental Technologies under Grant CSSET24EG01. We acknowledge the Nanosystem Fabrication Facility (CWB, HKUST) for the device fabrication.

Notes and references

1 Z. Basharat, N. S. Bayleyegn, M. A. Belete, O. O. Bello, D. T. Araki, J. A. Bielicki, C. S. Brown, E. Chung, R. M. Chandika, V. K. Chattu, D. T. Chu, O. Dadras, S. D. Darcho, S. Das, A. Gershberg Hayoon, B. F. R. Dickson, S. G. Djorie, S. Dohare, O. P. Doshi and S. Azadnajafabad, *Lancet*, 2024, **404**, 1199–1226.
2 J. N. Longfield, T. R. Townsend, D. F. Cruess, M. Stephens, C. Bishop, E. Bolyard and E. Hutchinson, *Infect. Control*, 1985, **6**, 445–450.
3 J. Kluytmans, *J. Hosp. Infect.*, 2007, **65**, 100–104.
4 S. Nayak, N. R. Blumenfeld, T. Laksanasopin and S. K. Sia, *Anal. Chem.*, 2017, **89**, 102–123.
5 T. Lehnert and M. A. M. Gijs, *Lab Chip*, 2024, **24**, 1441–1493.
6 A. Van Belkum and O. Rochas, *Front. Microbiol.*, 2018, **9**, 1437.
7 A. Rubio-Monterde, L. Rivas, M. Gallegos, D. Quesada-González and A. Merkoçi, *Microchim. Acta*, 2024, **191**, 638.
8 S. Zhang, S. Wang, B. Sun, S. Chen, Q. Ma, K. Han, C. Yin, X. Wang, H. Jiang and A. Merkoçi, *Sens. Actuators, B*, 2025, **425**, 137000.

9 R. Sista, Z. Hua, P. Thwar, A. Sudarsan, V. Srinivasan, A. Eckhardt, M. Pollack and V. Pamula, *Lab Chip*, 2008, **8**, 2091–2104.
10 F. Shen, W. Du, E. K. Davydova, M. A. Karymov, J. Pandey and R. F. Ismagilov, *Anal. Chem.*, 2010, **82**, 4606–4612.
11 D. L. House, C. H. Chon, C. B. Creech, E. P. Skaar and D. Li, *J. Biotechnol.*, 2010, **146**, 93–99.
12 E. A. Oblath, W. H. Henley, J. P. Alarie and J. M. Ramsey, *Lab Chip*, 2013, **13**, 1325–1332.
13 Y. H. Liu, C. H. Wang, J. J. Wu and G. B. Lee, *Biomicrofluidics*, 2012, **6**, 34119.
14 Y. D. Ma, K. H. Li, Y. H. Chen, Y. M. Lee, S. T. Chou, Y. Y. Lai, P. C. Huang, H. P. Ma and G. B. Lee, *Lab Chip*, 2019, **19**, 3737–3910.
15 C. H. Wang, K. Y. Lien, J. J. Wu and G. B. Lee, *Lab Chip*, 2011, **11**, 1521–1531.
16 G. Huang, Q. Huang, L. Xie, G. Xiang, L. Wang, H. Xu, L. Ma, X. Luo, J. Xin, X. Zhou, X. Jin and L. Zhang, *Sci. Rep.*, 2017, **7**, 6441.
17 K. G. Shah, M. Roller, S. Kumar, S. Bennett, E. Heiniger, K. Looney, J. Buser, J. D. Bishop, P. Yager and P. P. Banada, *PLoS One*, 2023, **18**, e0284424.
18 I. Choopara, A. Suea-Ngam, Y. Teethaisong, P. D. Howes, M. Schmelcher, A. Leelahavanichkul, S. Thunyaharn, D. Wongsawaeng, A. J. deMello, D. Dean and N. Somboonna, *ACS Sens.*, 2021, **6**, 742–751.
19 A. Suea-Ngam, I. Choopara, S. Li, M. Schmelcher, N. Somboonna, P. D. Howes and A. J. deMello, *Adv. Healthcare Mater.*, 2021, **10**, e2001755.
20 X. Meng, G. Zhang, B. Sun, S. Liu, Y. Wang, M. Gao, Y. Fan, G. Zhang, G. Shi and X. Kang, *Front. Microbiol.*, 2020, **11**, 1487.
21 J. Wen, L. A. Legendre, J. M. Bienvenue and J. P. Landers, *Anal. Chem.*, 2008, **80**, 6472–6479.
22 Y. Bu, S. Ni and L. Yobas, *Anal. Chem.*, 2023, **95**, 16453–16458.
23 V. N. Kondratova, O. I. Serd'uk, V. P. Shelepov and A. V. Lichtenstein, *BioTechniques*, 2005, **39**, 695–699.
24 A. Rogacs, L. A. Marshall and J. G. Santiago, *J. Chromatogr. A*, 2014, **1335**, 105–120.
25 R. B. Schoch, M. Ronaghi and J. G. Santiago, *Lab Chip*, 2009, **9**, 2145–2152.
26 W. Ouyang, Z. Li and J. Han, *Anal. Chem.*, 2018, **90**, 11366–11375.
27 W. Ouyang and J. Han, *Am. Ethnol.*, 2020, **59**, 10981–10988.
28 P. Agrawal, Z. Bognár and K. D. Dorfman, *Lab Chip*, 2018, **18**, 955–964.
29 D. J. Broemeling, J. Pel, D. C. Gunn, L. Mai, J. D. Thompson, H. Poon and A. Marziali, *J. Autom. Methods Manage. Chem.*, 2008, **13**, 40–48.
30 A. Marziali, J. Pel, D. Bizzotto and L. A. Whitehead, *Electrophoresis*, 2005, **26**, 82–90.
31 J. Pel, D. Broemeling, L. Mai, H. L. Poon, G. Tropini, R. L. Warten, R. A. Holt, A. Marziali and R. W. Davis, *Proc. Natl. Acad. Sci. U. S. A.*, 2009, **106**, 14796–14801.
32 S. Schmedes, P. Marshall, J. L. King and B. Budowle, *Int. J. Legal Med.*, 2013, **127**, 749–755.
33 J. Rousseau, G. Drouin and G. W. Slater, *Electrophoresis*, 2000, **21**, 1464–1470.
34 C. Heller, T. Duke and J. L. Viovy, *Biopolymers*, 1994, **34**, 249–259.
35 T. Ezaki and S. Suzuki, *J. Clin. Microbiol.*, 1982, **16**, 844–846.
36 E. K. Heiniger, J. R. Buser, L. Mireles, X. Zhang, P. D. Ladd, B. R. Lutz and P. Yager, *J. Microbiol. Methods*, 2016, **128**, 80–87.
37 M. Goto, E. Honda, A. Ogura, A. Nomoto and K. I. Hanaki, *BioTechniques*, 2009, **46**, 167–172.
38 X. Zhang, S. B. Lowe and J. J. Gooding, *Biosens. Bioelectron.*, 2014, **61**, 491–499.
39 B. Pang, S. Yao, K. Xu, J. Wang, X. Song, Y. Mu, C. Zhao and J. Li, *Anal. Biochem.*, 2019, **574**, 1–6.
40 X. Nie, *Plant Dis.*, 2005, **89**, 605–610.
41 N. Tomita, Y. Mori, H. Kanda and T. Notomi, *Nat. Protoc.*, 2008, **3**, 877–882.
42 O. Yeni, M. Şen, S. Hasançebi and N. Turgut Kara, *Sci. Rep.*, 2024, **14**, 23224.
43 M. Stegger, P. S. Andersen, A. Kearns, B. Pichon, M. A. Holmes, G. Edwards, F. Laurent, C. Teale, R. Skov and A. R. Larsen, *Clin. Microbiol. Infect.*, 2012, **18**, 395–400.
44 C.-H. Liu, C.-A. Chen, S.-J. Chen, T.-T. Tsai, C.-C. Chu, C.-C. Chang and C.-F. Chen, *Anal. Chem.*, 2019, **91**, 1247–1253.
45 I. Michael, D. Kim, O. Gulenko, S. Kumar, S. Kumar, J. Clara, D. Y. Ki, J. Park, H. Y. Jeong, T. S. Kim, S. Kwon and Y.-K. Cho, *Nat. Biomed. Eng.*, 2020, **4**, 591–600.
46 M. Sinha, J. Jupe, H. Mack, T. P. Coleman, S. M. Lawrence and S. I. Fraley, *Clin. Microbiol. Rev.*, 2018, **31**, e00089-17.
47 L. G. Reimer, M. L. Wilson and M. P. Weinstein, *Clin. Microbiol. Rev.*, 1997, 444–465.
48 L. A. Mermel and D. G. Maki, *Ann. Intern. Med.*, 1993, **119**, 270–272.
49 A. Afshari, J. Schrenzel, M. Ieven and S. Harbarth, Bench-to-Bedside Review: Rapid Molecular Diagnostics for Bloodstream Infection - a New Frontier?, *Crit. Care*, 2012, **16**, 222.
50 M. Pilecky, A. Schildberger, D. Orth-Höller and V. Weber, *Diagn. Microbiol. Infect. Dis.*, 2019, **94**, 7–14.
51 T. AbdElFatah, M. Jalali, S. G. Yedire, I. I. Hosseini, C. del Real Mata, H. Khan, S. V. Hamidi, O. Jeanne, R. S. Moakhar, M. McLean, D. Patel, Z. Wang, G. McKay, M. Yousefi, D. Nguyen, S. M. Vidal, C. Liang and S. Mahshid, *Nat. Nanotechnol.*, 2023, **18**, 922–932.
52 X. Fang, H. Chen, S. Yu, X. Jiang and J. Kong, *Anal. Chem.*, 2011, **83**, 690–695.
53 B. Crego-Vicente, M. D. del Olmo, A. Muro and P. Fernández-Soto, *Int. J. Mol. Sci.*, 2024, **25**, 6374.